PTEP

Prog. Theor. Exp. Phys. **2019**, 033B02 (16 pages)
DOI: 10.1093/ptep/ptz006

On experimental confirmation of the corrections to Fermi's golden rule

K. Ishikawa[1,2,*], O. Jinnouchi[3], A. Kubota[3], T. Sloan[4], T. H. Tatsuishi[1], and R. Ushioda[3]

[1]*Department of Physics, Faculty of Science, Hokkaido University, Sapporo 060-0810, Japan*
[2]*Natural Science Center, Keio University*
[3]*Department of Physics, Faculty of Science, Tokyo Institute of Technology, Tokyo, Japan*
[4]*Department of Physics, Lancaster University, Lancaster, UK*
[*]E-mail: ishikawa@particle.sci.hokudai.ac.jp

Received October 27, 2018; Revised December 27, 2018; Accepted January 2, 2019; Published March 17, 2019

Standard calculations by Fermi's golden rule involve approximations. These approximations could lead to deviations from the predictions of the standard model, as discussed in another paper. In this paper we propose experimental searches for such deviations in the two-photon spectra from the decay of the neutral pion in the process $\phi \to \pi^+\pi^-\pi^0$ and in the annihilation of the positron from nuclear β decay.

Subject Index B39

1. The correction to Fermi's golden rule

In an interacting many-body system described by a Hamiltonian $H_0 + H_1$, a state evolves with a Schrödinger equation. A one-particle state is specified by the momentum and non-interacting energy defined by H_0; the transition by H_1 has been studied by Fermi's golden rule. Although these transitionshave received attention from researchers, those that do not conserve energy often arise when the approximations are taken into account. The Schrödinger equation includes these approximations, which affect transitions of any states. Surprisingly, a correction term beyond Fermi's golden rule emerges. The correction becomes manifest in a transition of a finite time interval, which reveals a different dependence on the time interval and on the energy difference. The correction terms could be identified from experimental data; however, this is not as simple as was naively thought, for several reasons. One reason is that those signals that are caused by the corrections terms are similar to those of the experimental background. In the majority of cases they were considered as the background, and discarded. Another reason is the difficulty of finding the absolute value of the physical quantity in experiments, because the data is always modified by the efficiency of the detector. The transition rate describes the average behavior [1,2] of the process, and the correction terms give the dominant contribution to rapidly changing processes. Direct observation of these events might give the signals of the correction terms, but has not been possible up to the present. In general, it is difficult to separate these from the real background.

Accordingly, the correction terms were not a major concern for researchers. Nevertheless, the correction is one part of the total probability and contributes to natural phenomena. Fitting these experiments in an approximate way without the correction term might be possible and viable for a certain period; however, that could lead to serious inconsistency or an incorrect outcome at a later

Funded by SCOAP[3]

time, which must be avoided. It is thus important to confirm the existence of the correction term with simple and clean experiments.

Two-photon processes of the neutral pion and positron annihilation supply precise information on the transitions, and could be candidates. The rates are well understood theoretically, and have been determined from various experiments, in which the background has been subtracted. There are subtleties in the background subtraction, and the signal of the correction term has been insignificant. The correction terms are computed in a separate paper [3], and are found to be sizable. Due to their unusual properties, which will be presented later, it is not an easy task to disentangle them from the real background. Nevertheless, they give universal contributions to the phenomena. It will be shown that these are feasible in a ϕ-factory for the pion and in nuclear beta decays for the positron.

The neutral pion, π^0, is the lightest hadron composed of a quark and an anti-quark, and supplies much information on particle physics [4]. The rate of π^0 decay to two photons [5,6] is proportional to the number of colors N_c [7,8], and a measurement of its life time of $\tau = 10^{-16}$ s determined that $N_c = 3$. Despite this remarkable success, the average life time obtained from various methods [9] has a large uncertainty of about 10%. Accordingly, K-meson decays to two or three pions also have large uncertainties [4]. A large uncertainty also arises in the decay of para-positronium, which is a bound state of the electron and positron in quantum electrodynamics (QED). Its properties and transition rates are understood well, but the precision is not very good. The large uncertainty of the experimental values may suggest a fundamental problem in the transition probability.

We find the many-body wave function $|\Psi\rangle$ composed of normalized states from the Schrödinger equation

$$i\hbar\frac{\partial}{\partial t}|\Psi\rangle = (H_0 + H_{\rm int})|\Psi\rangle, \tag{1}$$

where H_0 and $H_{\rm int}$ are the free and interaction parts, and compute the rigorous transition amplitude. Hereafter we employ the natural units $\hbar = c = 1$ unless otherwise stated. The transition probability from a state $|i, 0\rangle$ at $t = 0$ to a state $|f, T\rangle$ at $t = T$ is determined by von Neumann's fundamental principle of quantum mechanics (FQM) as $P(T) = |\langle f, T|i, 0\rangle|^2$ for normalized states. For $P(T) \ll 1$, the average rate $\Gamma = \frac{P(T)-P(T_i)}{T-T_i}$ between a small T_i and a large T is given from the ratio of fluxes of outgoing waves over that of incident waves, and is in agreement with that derived from the golden rule for the final state of a continuous spectrum. In these standard calculations, plane waves and interactions that switch off adiabatically (ASI) are used. Although this value has been used in the majority of processes, experiments are made with finite time intervals, and the value is measured without an average.

Theoretical values under these conditions are necessary. Stueckelberg studied this problem some time ago and found that the transition amplitudes of the plane waves for a finite time interval lead to a divergence [10], even at the tree level. This is not connected with the ultraviolet divergences due to the intermediate states, but to non-normalized initial and final states. It is possible to avoid this difficulty by using normalized states. Those computed in the previous paper, Ref. [3], are applied to experiments.

$P(T)$ at a large T is the sum

$$P(T) = \Gamma T + P^{(d)}, \qquad P^{(d)} = P(T_i) - \Gamma T_i, \tag{2}$$

where T_i is determined by the time at which the initial wave packets separate, determined by $\sqrt{\sigma}_i$, where σ_i is the spatial size of the initial wave. At $\Gamma T_i < 1$, and at $T > T_i$, $P^{(d)}$ is constant.

Γ is computed with the standard S-matrix $S[\infty]$ under ASI [11–13], but $P^{(d)}$ is computed with the wave functions following FQM [14–17]. A rigorous probability will be obtained without facing the difficulty raised by Stueckelberg by using wave packets instead of plane waves.

Experimental proof of $P^{(d)}$ in neutral pion decay, positronium decay, and positron annihilations are studied. Two-photon decay of para-positronium is almost equivalent to neutral pion decay. Their systematic analyses are presented. It will be shown that the unique properties derived from the probability $\Gamma T + P^{(d)}$ can be confirmed experimentally.

The paper is organized as follows: In Sect. 2 pion decay is analyzed, and in Sect. 3 positron annihilation is analyzed. In Sect. 4, the wave packet sizes and relevant parameters are estimated. In Sect. 5, the experiments are studied and a summary and prospects for the future are presented. Appendix A is devoted to various formulae, and Appendix B describes a method for entanglement of the accidental background.

2. Two-photon decay of the neutral pion

The interactions of a neutral pion or para-positronium with two photons are derived from the triangle diagram of the quark or the electron as $L_{\rm int} = -g\,\varphi\,\epsilon_{\mu\nu\rho\sigma}F^{\mu\nu}F^{\rho\sigma}$, in which the coupling for the pion is $g = \frac{\alpha}{4\pi f_\pi}$, which is almost constant from the confining mechanism and is related to the $\pi\gamma\gamma$ coupling [7,8]. For the positronium, the binding energy is small and the coupling varies with the momentum, which will be ignored for a while. Substituting this into Eq. (1), we have the transition amplitude for an initial state of the central momentum and position into two photons,

$$\mathcal{M} = \int_{T_\pi}^{T_\gamma} dt \int d^3x \langle K_1, X_1; K_2, X_2 | H_{\rm int}(x) | P_\pi, X_\pi \rangle. \tag{3}$$

A Gaussian wave packet [14,18–20] satisfies the minimum uncertainty, which is ideal for studying a transition of a finite time interval, and is used in the majority of places. A non-Gaussian form is also physically relevant, and is studied later. Wave packets of size σ_i with the central momentum and position $E_A = \sqrt{P_A^2 + m_A^2}$ and $E(K_i) = |K_i|$, where $i = 1, 2$ and $\vec{V}_A = \frac{\vec{P}_A}{E_A}$ is the group velocity of the momentum $\vec{P}_A$, are used throughout this paper, and the upper-case roman letters $A, B, \ldots$ run over $\pi, 1, 2$ so that, e.g., $\sum_A$ stands for $\sum_{A=\pi,1,2}$, etc. An imaginary part is added to the energy of the unstable initial state according to Refs. [21,22]; see also Ref. [11] for a review. Integration over the space position leads to a Gaussian function in the momentum difference, and integration over time leads to[1]

$$\mathcal{M} = N_0(\vec{X}_i)\epsilon_{\mu\nu\rho\sigma}\epsilon^\mu(K_1)K_1^\nu\epsilon^\rho(K_2)K_2^\sigma e^{-\frac{\sigma_s}{2}(\delta P)^2} G(\delta\omega), \tag{4}$$

where $N_0(\vec{X}_i)$ shows a dependence on the positions, $\delta P = P_\pi - K_1 - K_2$, $\delta\omega = E_\pi - E_1 - E_2 - \vec{V}_0\delta P$, $\sigma_s = \left(\sum_A \frac{1}{\sigma_A}\right)^{-1}$, and $G(\delta\omega)$ is expressed with the error function $\mathrm{erf}(x+iy)$. Their explicit forms are given in Ref. [3]. The transition probability is written as

$$P = \frac{1}{2}\int d^3X_1 d^3X_2 \frac{d^3K_1}{(2\pi)^3}\frac{d^3K_2}{(2\pi)^3}\left|N_0(\vec{X}_i)\right|^2 2\,(K_1\cdot K_2)^2\, e^{-\sigma_s(\delta P)^2}\,|G(\delta\omega)|^2\,. \tag{5}$$

[1] We have put the central momentum K_i in the polarization ϵ^μ and in the derivative interaction. See Ref. [17] for a justification.

As shown in Ref. [3] in detail, $G(\delta\omega)$ depends on an intersection of the trajectories determined by the positions of $\vec{X}_i$, $i = 1, 2$. If they intersect outside of the material, the interaction does not occur and the amplitude vanishes; if inside the material, the interaction occurs. This is a bulk region. In the boundary region, the interaction partly occurs. This is the boundary region.

Integration in the bulk is proportional to the time interval due to the translational invariance along the initial momentum, and that in the boundary is proportional to the width of the boundary region, σ_t, which depends on the wave packet size and the velocity variation, $\sigma_t = \frac{\sigma_s}{\Delta V^2}$. The derivation is given in Ref. [3].

The momentum distribution is written as a sum of two terms,

$$\frac{dP}{d^3K_1 d^3K_2} = 2\,(K_1 \cdot K_2)^2\, e^{-\sigma_s(\delta P)^2} \sum_{k=\text{bulk,boundary}} P_0^k \left| G^k(\delta\omega) \right|^2, \tag{6}$$

with

$$P_0^k = \begin{cases} g^2 2^{-6} (\sigma_\pi)^{3/2} (E_\pi E_1 E_2)^{-1} C \tau_\pi \left(1 - e^{-\frac{T}{\tau_\pi}}\right) & \text{for bulk,} \\ g^2 2^{-6} (\sigma_\pi)^{3/2} (E_\pi E_1 E_2)^{-1} C \sqrt{2\sigma_t} & \text{for boundary,} \end{cases} \tag{7}$$

where $T = T_\gamma - T_\pi$, and C is a constant of energy dimension E^1 that depends on the wave packet parameters. The square of $G(\delta\omega)$ in the asymptotic region is

$$|G^k(\delta\omega)|^2 = \begin{cases} \frac{1}{\frac{1}{\sigma_t} + (\delta\omega)^2}, & \text{from boundary } (\frac{\sigma_t}{2}\delta\omega^2 \gg 1), \\ 2\pi\sigma_t e^{-\sigma_t(\delta\omega)^2} & \text{from the bulk } (\frac{\sigma_t}{2}\delta\omega^2 \ll 1), \end{cases} \tag{8}$$

where T_0^R is the time at which the wave packets intersect. The bulk term decreases rapidly with $\delta\omega$, and the boundary term decreases slowly with an inverse power of the energy difference.

In the decay of a high-energy pion of $p_\pi = (E_\pi, 0, 0, p_\pi)$, the momenta of the final states are almost parallel to the pion. In the boundary term, $|G(\delta\omega)|^2$ decreases slowly as $K_i \to \infty$, and leads to a large contribution to the probability.

In the transition, the total energy is conserved but the kinetic energy is partly violated. The bulk contribution is narrow in the kinetic energy, and reveals the golden rule. The boundary contribution is broad in the kinetic energy, and reveals the correction term. The deviation of the kinetic energy from the total energy is the interaction energy $V_{\text{int}} = \langle\Psi|H_{\text{int}}|\Psi\rangle$. The coupling strength g can be treated as constant for the golden rule, where $k_{\gamma_i} \cdot k_{\gamma_{i'}} \ll m_q$. However, the boundary term is spread in the wide kinetic region of $k_{\gamma_i} \cdot k_{\gamma_{i'}}$, which includes the region $k_{\gamma_i} \cdot k_{\gamma_{i'}} \gg m_q^2$. There, this coupling strength becomes a function of $k_{\gamma_i} \cdot k_{\gamma_{i'}}$, $g(k_{\gamma_i} \cdot k_{\gamma_{i'}})$, behaving as [23]

$$g(k_{\gamma_i} \cdot k_{\gamma_{i'}}) = g \frac{m_q^2}{2k_{\gamma_i} \cdot k_{\gamma_{i'}}}. \tag{9}$$

Here, m_q is the composite quark mass of magnitude around $\frac{m_p}{3}$, where m_p is the proton's mass. Thus $P^{(d)}$ becomes maximum at around $k_{\gamma_i} \cdot k_{\gamma_{i'}} \approx \frac{m_p^2}{2}$. Its magnitude is proportional to the proton's mass. This behavior shows that the average interaction energy $\langle|H_{int}|\rangle$ is the order of the proton's rest energy, m_p.

For a high-energy pion, the initial and final waves overlap in a wide area for photons propagating in the direction parallel to the pion. The boundary region becomes large in size, and gives a large contribution to the probability.

3. Positron annihilation

Positrons and electrons are described by the field $\psi(x)$, and a photon by $A_\mu(x)$, in QED, and the interaction is $e\bar{\psi}(x)\gamma_\mu\psi(x)A^\mu(x)$. Para-positronium decay and free positron annihilation are derived from this interaction; the former is also expressed by an effective interaction equivalent to the pion two-photon interaction. The latter is described by the second-order perturbative expansion with respect to the above interaction. $P(T)$ in these decays is studied below.

3.1. Para-positronium decay

Para-positronium is even in charge conjugation and decays to two photons. The formula of the decay probability in Eq. (6) is applied after changing the parameters to suitable ones. The average life time of para-positronium is much longer than that of the pion, and the wave packet size is also longer. Positronium decays and positron annihilation in porous material, which is composed of small holes and many boundary regions, are analyzed. We will see that the boundary term is enhanced.

3.2. Free positron annihilation

The annihilation amplitude of a free positron and free electron at rest for the central values of momentum and position

$$\chi_{e_i} = (\vec{p}_{e_i}, \vec{X}_{e_i}, \sigma_{e_i}), \quad \chi_{\gamma_i} = (\vec{p}_{\gamma_i}, \vec{X}_{\gamma_i}, \sigma_{\gamma_i}) \tag{10}$$

for the photons, the electron, and the positron are

$$\mathcal{M} = \langle \chi_{\gamma_1}; \chi_{\gamma_2} | \int_0^T dx_1 \int_0^{t_1} dx_2 H_{\rm int}(x_1) H_{\rm int}(x_2) | \chi_{e_1}, \chi_{\bar{e}_2} \rangle, \tag{11}$$

where T is the time interval for which the positron crosses a grain of the target. The integrations over the coordinates $\vec{x}_i$ and over the momentum $\vec{q}$ for the intermediate state are made using Gaussian integrations.

Integration over time gives the bulk and boundary terms, and leads to the amplitude being written as in Eq. (4). Substituting these, we have the momentum distribution

$$\begin{aligned}\frac{1}{TL^3}\frac{dP}{d^3k_1 d^3k_2} = \frac{2}{m^2}\left(1 + \frac{1}{4}(1-\cos\theta) + \frac{1}{2}\left(\frac{m}{E_{\gamma_1}} + \frac{m}{E_{\gamma_2}}\right)\right) \\ \left[e^{-\sigma_s(\delta P)^2}\left(P_0^{\rm bulk}\,|G_{\rm bulk}(\delta\omega)|^2 + P_0^{{\rm b}_t}\left|G_{{\rm boundary}_{(t)}}(\delta\omega)\right|^2\right)\right. \\ \left. + P_0^{{\rm b}_s} e^{-\sigma_s(\delta P)^2}\left|G_{{\rm boundary}_{(s)}}(\delta\omega)\right|^2\right],\end{aligned} \tag{12}$$

where Eqs. (A.22) and (A.12) are substituted, and

$$P_0^{\rm bulk} = (E_{e^+}E_{\gamma_1}E_{\gamma_2})^{-1}C \qquad \text{bulk}, \tag{13}$$

$$P_0^{{\rm b}_{(t)}} = (E_{e^+}E_{\gamma_1}E_{\gamma_2})^{-1}C\frac{\sqrt{2\sigma_t}}{T} \qquad \text{boundary in time}, \tag{14}$$

$$P_0^{{\rm b}_{(s)}} = (E_{e^+}E_{\gamma_1}E_{\gamma_2})^{-1}C\frac{\sqrt{2\sigma_t 2\sigma_s}}{TL} \qquad \text{boundary in space}, \tag{15}$$

where C is a constant [3]. In silica powder, this size is semi-microscopic, of the order of a few nanometers, and almost the same or slightly larger than $\sqrt{\sigma_\gamma}$. In the present situation, the target is

composed of silica particles of $L = 7$ nm, and it is reasonable to assume that the ratios $\frac{\sqrt{2\sigma_s}}{L}$ and $\frac{\sqrt{2\sigma_t}}{T}$ are $\frac{1}{10}$–$\frac{1}{100}$. The positron energy is $E_{e^+} = m_e$ with an energy uncertainty of 10%. The spectrum of the boundary term is of the universal form, but its magnitude has uncertainties due to the uncertainties on the wave packets. This ambiguity could be studied by a light scattering of the silica powder.[2]

4. Initial and final states

We apply the decay probability of Eq. (6) to the neutral pion in the process

$$e^+ + e \to \phi \to \pi^+ + \pi^- + \pi^0, \tag{16}$$

and that of the positron in Eq. (12) in the process

$$^{22}\mathrm{Na} \to {}^{22}\mathrm{Ne}^* + e^+ + \nu, \quad {}^{22}\mathrm{Ne}^* \to {}^{22}\mathrm{Ne} + \gamma. \tag{17}$$

The former experiment is made in a high-energy laboratory, and the latter experiment is made in a low-energy laboratory.

4.1. Wave packet shape and size

The total transition rate Γ derived from Eqs. (6) and (12) is independent of the wave packet parameters. This is consistent with the general theorem given by Stodolsky [24–27][3] on stationary physical quantities. This theorem, however, is not applied to a non-stationary quantity such as $P^{(d)}$. In fact, $P^{(d)}$ derived from Eqs. (6) and (12) depends on the forms and sizes of the wave packets. Until now, the Gaussian wave packet, which decreases exponentially in position and momentum and satisfies the minimum uncertainty $\delta x \delta p = \hbar$ and $\delta p = 0$ for $\delta x = \infty$, has been used. This is ideal for studying the transition for a finite time interval. Other wave packets satisfying $\delta x \delta p \geq \hbar$ are shown to lead to almost equivalent results. σ_π, σ_γ, and $\sigma_{\bar{e}}$ represent σ_s for the pion, photon, and positron, respectively.

These particles interact with microscopic objects in matter and cause the final states to be produced, from which a number of the events and the probability are determined. Accordingly, the packet parameters in our formulae are determined by these states in matter. This method has been shown to be valid in Refs. [14–17], and in the quantum transition of two atoms in an energy transfer process in photosynthesis [28].

4.1.1. Sizes of wave functions: π^0

σ_{π_0}: In order for the electron and the positron to produce a ϕ meson, they are accelerated from the average electron momentum in matter, which is less than $\frac{1}{10^{-10}\,\mathrm{m}}$. The relaxation time for these electrons and positrons in matter, beyond which they lose coherence due to environmental effects, is around 10^{-14} s, which corresponds to the mean free path of 3×10^{-6} m for the speed of light, and is slightly shorter at lower energy. Values of 10^{-14} s and 10^{-7} m for the spatial electron sizes in matter are used. The positron is produced by the electron collision with matter, and the length is the same as that of the electrons. During their acceleration, the time interval that the wave packets pass through a spatial position is kept unchanged. Although the amplitude of three pions,

[2] A raman scattering experiment has seen anomalous signals. Private communications from Professor M. Takesada.

[3] Reference [24] and other works studied the neutrino oscillation amplitude within the golden rule in the wave packet formalism. See Refs. [25,26] for recent references.

which is described by the intermediate ϕ meson of the Breit–Wigner form of the energy width of few MeV, peaks around the central energy, if the initial state has a fixed energy, each pion can have infinitesimal energy uncertainty. Accordingly, the width of the ϕ meson is related neither to the uncertainty of the pion's energy nor to the pion's wave packet size. Nevertheless, the above relaxation time of the electron and positron results in an uncertainty in the three pion's energy of a few meV. Thus the energy uncertainty of π^0 is governed by the relaxation time. That leads to 3×10^{-6} m for π^0 in the present process.

σ_γ in π^0 decay: The detection process of the photon is governed by its reaction with the atoms, and the following coherent transitions by which electronic signals emerge in the detector. They occur within the finite spatial area occupied by the wave functions in the solid. The transition amplitude of the photon is described by a wave packet of this size. Thus, σ_γ represents the spatial size of the electron wave function in the configuration space that the photon interacts with. The initial process depends on the energy. For an energy of 0.5 GeV, the majority of the events are pair production due to the nucleus electric field. Accordingly, $\sigma_\gamma = \frac{s_\gamma}{m_\pi^2}$, where $s_\gamma \leq 1$, and $s_\gamma = 0.5$ is used for the following estimation.

σ_γ and T_i derived from σ_i govern the magnitude of $P^{(d)}$. For high-energy colliding beam experiments, the sizes of the positron and the electron are determined by the spatial size of the electron wave function in matter; $T_i = 10^{-14}$ s from the relaxation time, and $\tau = 10^{-16}$ s.

At the time interval $T \gg \tau = \frac{1}{\Gamma}$, the ratio $T_i\Gamma$ becomes $\frac{T_i}{\tau}$. Now, $c\tau$ is 10^{-8} m. Accordingly, the ratio $\frac{T_i}{\tau} m_\pi^2 \sigma_\gamma \frac{1}{64} = \frac{10^{-14}}{10^{-16}} \times 0.5 \times \frac{1}{64} = 0.8$. From this value the probability that one of the photons is in the energy range around the central energy ${E_\gamma}^0$, $\frac{E_\gamma - {E_\gamma}^0}{{E_\gamma}^0} \leq 0.1$, is about 10%. This would be consistent with the current uncertainty of the neutral pion's average life time.

4.1.2. Sizes of wave functions: $\bar{e}$

σ_{e^+}: First we study the spatial size of the positron wave packet for a process where the gamma from positron annihilation is measured. ^{22}Na is at rest and bound in matter. The spatial extension of the ^{22}Na wave function in the configuration space would be $\frac{1}{2000}$ of the electron wave function from the ratio of the masses. A positron emitted from ^{22}Na decay has this size in the direction perpendicular to its momentum, and that in the parallel direction can be much longer. This loses the energy in matter on average 10^{-12} s [29]. Hence the time interval in which the positron wave function keeps coherence, or the average relaxation time, is 10^{-12} s.

The wave packet size for a detected positron is estimated based on the detector used. When a plastic scintillator containing benzene is used, the spatial size of the benzene molecule, around 1 nm, shows the positron wave packet size.

σ_{Ps}: Positronium is formed in porous material and decays there. The size of the porous material determines the effective size of the interaction area, and determines the time interval of the transition amplitude.

σ_γ in positron annihilation: The dominant process of the photon with matter in a detector in this energy region, around a few hundred keV, is the photo-electric effect, in which the photon excites an atom. The relevant spatial size is the size of the atom, which is characterized by $\pi \times (\frac{a_\infty}{2})^2$, where $a_B = \frac{1}{m_e \alpha}$ is the Bohr radius. Excited atoms make successive transitions and produce many photons, electrons, and ions of low energy. These processes are expressed by the time-dependent Schrödinger equation which describe the electrons, photons, and ions. These states are expressed by the wave functions of finite spatial extensions, wave packets. The size of the coherent area of

these wave functions would be of the order of a few atomic sizes, due to decoherence caused by many atoms. The wave packet size, σ_γ, of the photon may be of a few atomic sizes. The parameters may depend on the detector [30,31].

4.2. Boundary regions

The wave functions of the electron and positron overlap at the boundary region of the matter, and their annihilation takes place. The area is large, and the events increase in porous material. The porous material size determines the effective size of the area and the time interval of the transition. The transition amplitudes and probabilities depend on these sizes. This is used in positron experiments.

For experiments that use small powders, electrons are inside the small region, and the interaction takes place in the inside or at the boundary region. The transition amplitudes and probabilities depend on these sizes.

4.3. Energy resolution

An ideal detector that detects and gives the energy of a particle or a wave directly does not exist. For its measurement, signals caused by its reactions with matter are read first and converted to the energy using a conversion rule justified by other processes. The energy is measured with finite uncertainty. This is the energy resolution, and all detectors have finite energy resolution. This causes an experimental uncertainty. The energy resolution, $\sigma(E)$, has both statistical and intrinsic origins, which is written as

$$\sigma(E) = \sigma_{\text{statistics}}(E) + \sigma_{\text{intrinsic}}(E), \tag{18}$$

where $\sigma_{\text{statistics}}(E)$ is normally determined from Poisson statistics and the other is written as $\sigma_{\text{intrinsic}}(E)$, in which an effect due to the finite size of wave functions, Eq. (5), is included. The former depends on the detector's type, and the latter does not and has universal properties regardless of detector type. In a scintillation detector, the electric signal of a γ-ray is obtained according to the number of scintillation photons N, and the energy resolution, $\sigma_{\text{statistics}}(E)$, is given by

$$\sigma_{\text{statistics}}(E) = 2.35\sqrt{\frac{F}{N}}E, \tag{19}$$

where N is the number of samples and F is a correction factor, the Fano factor. For NaI(Tl), $F = 1$ $\sigma_{\text{statistics}}(E)/\langle E\rangle$ is around 5%–10%, and the energy resolution is 25–50 keV for an energy of 500 keV. A Ge detector has a different mechanism of much smaller statistical uncertainty, due to a small F and large N. The distribution around the central value decreases exponentially with E.

The wave packet size determined by the size of the atom is $\pi(10^{-10})^2\,\text{m}^2$, and should be almost the same in NaI(Tl) and Ge detectors; this leads to an energy uncertainty of $\sigma_{\text{intrinsic}}(E) = 1\,\text{keV}$. Accordingly, in NaI, $\sigma_{\text{statistics}}(E)$ is the dominant one and $\sigma_{\text{intrinsic}}(E)$ is negligible, but in a Ge detector, $\sigma_{\text{intrinsic}}(E)$ shares a substantial part.

4.4. Energy distribution

The energy distributions of the bulk term and the boundary term are very different. That from Γ for plane waves under ASI is proportional to $\delta(E_i - E_f)$, but for wave packets it behaves as $e^{-(\frac{\delta\omega}{\sigma(E)})^2}$, where the width is of a universal nature and behaves differently from that of the statistical case. That of $P^{(d)}$ decreases in E^{-n}, where $n \geq 0$ depends on the decay dynamics. $P^{(d)}$ can be identified easily in the energy region $E \gg \sigma(E)$ if the relative fraction over ΓT is of substantial magnitude, of

the order of 10^{-3} or larger, even with a detector of large energy resolution. Despite its large energy resolution, a NaI(Tl) scintillator is useful for the confirmation of $P^{(d)}$. A detector of much smaller resolution such as a Ge detector is also useful.

5. Experimental confirmation

As $P^{(d)}$ possesses many unusual properties, phenomena originating from $P^{(d)}$ reveal intriguing properties. By detecting these events, $P^{(d)}$ can be confirmed. Γ has been well established, and phenomena of Γ origin have been understood precisely with the help of numerical methods. They are compared with data from natural phenomena and observations. If clear disagreements are found, and if it is resolved by $P^{(d)}$, this may confirm $P^{(d)}$.

5.1. Magnitude of $P^{(d)}$

The magnitude of $P^{(d)}$ for para-positronium decay, $P^{(d)}(pp)$, and direct annihilation, $P^{(d)}(da)$, is estimated and given in Fig. 1. They depend on the size and shape of the wave packets. We use the value $\sigma_\gamma > 10^{-20}\,\mathrm{m}^2$ with a Gaussian wave function and power-law wave function, and find that

$$\begin{aligned} P^{(d)}(pp) &= 10^{-12} \quad \text{(Gaussian wave function)} \\ &= 3 \times 10^{-4} \quad \text{(power-law wave function)} \\ P^{(d)}(da) &= 2 \times 10^{-6} \quad \text{(Gaussian wave function)} \\ &= 3 \times 10^{-4} \quad \text{(power-law wave function).} \end{aligned}$$

At the moment we are not aware of the precise shape and size of the wave function. Light scattering may be useful to study the wave function.[2]

The photon distribution is modified by $P^{(d)}$ in positron annihilation and positronium decay. The high-energy side is not affected by the modified energy by Compton scatterings, which is not true on the low-energy side. By measuring multiple coincident photons in the high-energy regions, clear signals may be obtained. Although accidental coincident events may contribute, they can be separated and events of $P^{(d)}$ origin in the data estimated. It is our expectation that with 10^8 events of positron annihilation a confirmation of P^d could be in scope.

GEANT4 [32] is a simulation program that includes the transition probability and detector performance. The probabilities derived from the golden rule are employed. Hence, this is quite useful for analyzing natural phenomena, including a detector's response and backgrounds. Comparing the events derived from the golden rule of the standard theory with the observations, we are able to see if a non-standard component is included.

5.2. Backgrounds from decay (annihilation) in flight

The signals from decay or annihilation in flight are in energy regions different from those at rest, and give background. A positron loses its energy in an insulator in picoseconds [33], and stops. A photon produced before the stop has an energy higher than m_e and its contribution is estimated in two steps.

The average positron life time due to annihilation or decay is 100–500 ps, and depends on various conditions. Hereafter we use 200 ps for the average life time and 2 ps for the thermalization time. The ratio of annihilation events of positrons in flight over those at rest is less than $\frac{2}{200} = 10^{-2}$. The experimental value seems to be less than 10^{-3} or 10^{-4} [34]. Among the events of energy

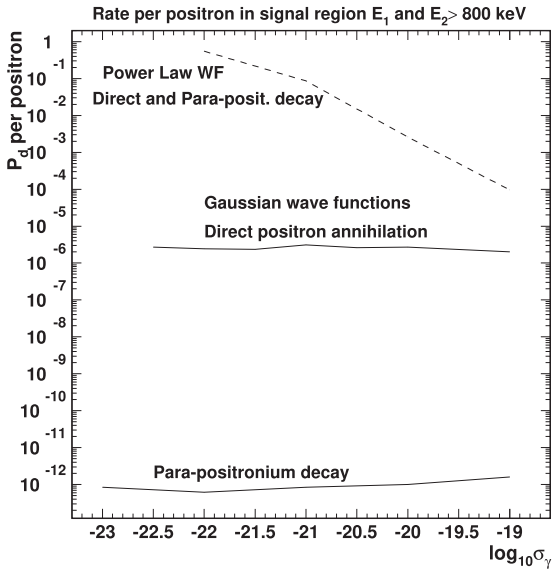

Fig. 1. The variation of the expected ratio of events per stopping positron in silica with σ_γ for different assumed situations. The upper curve shows the ratio if direct wave functions are dominant, the middle curve shows the ratio if direct annihilation dominates, and the lower curve if the annihilation is dominant through the decay of para-positronium.

$E_1 + E_2 > 2m_e c^2$, the fraction in the energy region $E_1 + E_2 - 2m_e c^2 \geq 3\sigma E$, where σE is the width of a NaI(Tl) detector, is obtained as $\frac{1}{230}$ from Bethe's formula [35]. A further suppression factor of $\frac{1}{10}$ is multiplied due to the specific configuration of the detector setup of the present experiment. Combining these numbers, the fraction is 0.43×10^{-6} or 0.43×10^{-7}. This gives the magnitude of the background from in-flight annihilation as less than 10^{-6}.

5.3. Uncertainties

Possible sources of uncertainties and ambiguities are matter effects, accidental coincident events (double hits), and environmental gammas.

The photon spectrum in the high-energy region is not modified by Moeller scattering, the photo-electric effect, the Compton effect, or pair production. Accordingly, matter effects are irrelevant. Environmental gammas or those of cosmic ray origin are avoided by selecting coincident events of multiple gammas. In the two-gamma case, coincidences between one gamma from Ne radiative decay and another from positron annihilation are taken. In the three-gamma case, coincidences between one gamma from ^{21}Ne* radiative decay and two photons from positron annihilation are taken. In these multiple coincident events, there remain accidental coincident events (double hits). Because their strength depends upon the initial positron flux, and the spectrum has different momentum dependence than the signal from $P^{(d)}$, it is possible to disentangle them following Appendix B.

5.4. Related processes

Para-positronium decay is included in the text. Another spin component, orth-positronium, may be used for a $P^d \neq 0$ test. However, orth-positronium has a much longer life time and $P^{(d)}$ becomes much smaller. Its effect is difficult to observe experimentally. $P^{(d)}$ in nuclear gamma and beta decays also becomes sizable, and can be non-vanishing even in processes of $\Gamma = 0$. Various selection rules are valid only for Γ, but not for $P^{(d)}$. The role of $P^{(d)}$ is therefore important.

6. Summary and prospects

$P^{(d)}$ can be confirmed experimentally from photon distributions.

(1) The energies of the photons in positron annihilation at rest from the golden rule satisfy $E_{\gamma_1} + E_{\gamma_2} = 2m_e$, whereas those from $P^{(d)}$ satisfy $E_{\gamma_1} + E_{\gamma_2} < 2m_e$ or $E_{\gamma_1} + E_{\gamma_2} > 2m_e$. The photon loses its energy by Compton scattering, and that produced by the golden rule can be detected in the former region, but not in the latter region. Events of energies $E_{\gamma_1} + E_{\gamma_2} > m_e$ are generated only by $P^{(d)}$, and may be worthwhile for its confirmation.
(2) For the neutral pion, our finding of $P^{(d)} \approx O(0.8)$ suggests that $P^{(d)}$ must be implemented for analysis. The previous large uncertainty of about 10% in the life time would be due to $P^{(d)}$, and will be reduced in an analysis that includes $P^{(d)}$.
(3) Tagging π^+ and π^- in the process $e + \bar{e} \to \phi$, $\phi \to \pi^+ + \pi^- + \pi^0$, the π^0 momentum is determined, and the photon spectrum is computed. Due to $P^{(d)}$, this spectrum deviates from the golden rule. If the deviation is observed, $P^{(d)}$ will be confirmed.
(4) Many-body wave functions of $\delta E = E_{\text{initial}} - (E_{\gamma_1} + E_{\gamma_2}) \neq 0$ have interaction energies that are independent of the frequency of each wave. This leads to an extra component to the energy momentum tensor in addition to those proportional to the frequencies. Normal detection processes measure the wave's frequencies, but not these interaction energies. Accordingly, this corresponds to an invisible energy. This state may be considered as a kind of halo.
(5) Once the confirmation of P^d is made, (i) methods to reduce current uncertainties in experiments, and (ii) mechanisms to solve current puzzling phenomena will be found.

Acknowledgements

This work was partially supported by a Grant-in-Aid for Scientific Research (Grant No. 24340043). The authors thank Dr. K. Hayasaka, Dr. K. Oda, and Mr. H. Nakatsuka for useful discussions.

Funding

Open Access funding: SCOAP[3].

Appendix

A. Free positron annihilation

A.1. Amplitude

The amplitude for a free positron annihilation is

$$M = \int_0^T dt_1 \int d^3x_1 \int_0^{t_1} dt_2 d^3x_2 \langle \gamma_1, \gamma_2 | H_{\text{int}}(x_1) H_{\text{int}}(x_2) | e, \bar{e} \rangle \tag{A.1}$$

$$= \frac{1}{2} \int_0^T dt_1 \int_0^T dt_2 d^3x_1 d^3x_2 \langle \gamma_1, \gamma_2 | T(H_{\text{int}}(x_1) H_{\text{int}}(x_2)) | e, \bar{e} \rangle, \tag{A.2}$$

where $H_{\text{int}}(x)$ is the interaction part of QED and the initial and final states are wave packets, and

$$T(H_{\text{int}}(t_1) H_{\text{int}}(t_2)) = \theta(t_1 - t_2) H_{\text{int}}(t_1) H_{\text{int}}(t_2) + \theta(t_2 - t_1) H_{\text{int}}(t_2) H_{\text{int}}(t_1). \tag{A.3}$$

Applying Wick's theorem,

$$\begin{aligned} M &= \sum :: \gamma_\mu S_F(x_1 - x_2)\gamma_\nu + \cdots \\ &= \bar{u}(p_1)\left[\gamma\epsilon(k_1)\frac{\gamma(p_1 - k_1) + m_e}{(p_1 - k_1)^2 - m_e^2}\gamma\epsilon(k_2) + \gamma\epsilon(k_2)\frac{\gamma(p_1 - k_2) + m_e}{(p_1 - k_2)^2 - m_e^2}\gamma\epsilon(k_1)\right]v(p_2) \\ &= -\bar{u}(p_1)\left[\frac{\gamma k_1\gamma\epsilon(k_1)\epsilon(k_2) + 2\epsilon(k_1)p_1\gamma\epsilon(k_2)}{2p_1k_1} + \frac{\gamma k_2\gamma\epsilon(k_2)\gamma\epsilon(k_1) + 2\epsilon(k_2)p_1\gamma\epsilon(k_1)}{2p_1k_2}\right]v(p_2), \end{aligned} \tag{A.4}$$

where

$$\bar{u}(p_1)\gamma\epsilon(k_1)(\gamma p_1 + m_e) = 2\epsilon(k_1)p_1\bar{u}(p_1) \tag{A.5}$$

and the similar one for the $v(p_2)$ were substituted. For $p_1 = (m, o),\ p_2 = (m, o)$, it follows that

$$\sum_{\text{spin}} |M|^2 = \frac{8}{m_e^2}\left[1 + \frac{1}{4}(1 - \cos\theta) + \frac{1}{2}\left(\frac{m}{k_1^0} + \frac{m}{k_2^0}\right)\right]. \tag{A.6}$$

Note that this is slightly different from that for positronium decays.

A.2. Boundary in space and time

A.2.1. Amplitude

In scatterings in the laboratory frame where the target is composed of small particles of volume L^3, the momentum-dependent amplitudes in the bulk and boundary terms of Eq. (15) are replaced with

$$M_{\text{bulk}} = \sqrt{2\pi\sigma_t}e^{-\frac{\sigma_t}{2}(\delta\omega)^2}(2\pi\sigma_s)^{3/2}e^{-\frac{\sigma_s}{2}(\delta\vec{p})^2}\theta(\vec{X}_\gamma, \text{volume}), \tag{A.7}$$

$$M_{\text{boundary}_{(t)}} = \sqrt{\frac{2\sigma_t}{\pi}}\frac{1}{-i\sqrt{\sigma_t}\delta\omega + 1}(2\pi\sigma_s)^{3/2}e^{-\frac{\sigma_s}{2}(\delta\vec{p})^2}\theta(\vec{X}_\gamma, \mathrm{b}_t), \tag{A.8}$$

$$M_{\text{boundary}_{(s)}} = \sqrt{\frac{2\sigma_t}{\pi}}\frac{1}{-i\sqrt{\sigma_t}\delta\omega + 1}(2\pi\sigma_s)^{2/2}\sqrt{\frac{2\sigma_s}{\pi}} \times \theta(\vec{X}_\gamma, \mathrm{b}_{(t,s)}) \tag{A.9}$$

$$\left[\frac{1}{-i\sqrt{\sigma_s}\delta p_z + 1}e^{-\frac{\sigma_s}{2}((\delta\vec{p}_x)^2 + (\delta\vec{p}_y)^2)} + (z, x, y) \to (x, y, z), (y, z, x)\right], \tag{A.10}$$

where $\theta(\vec{X}_\gamma, \text{volume})$, $\theta(\vec{X}_\gamma, \mathrm{b}_t)$, and $\theta(\vec{X}_\gamma, \mathrm{b}_{(t,s)})$ show that the intersections of trajectories are inside the volume L^3, in the boundary in time, and in the boundary in space and time.

The momentum-dependent term in the bulk, Eq. (21), and the boundary term in time, Eq. (22), lead to a probability of the same form as before,

$$|G_{\text{bulk}}(\delta\omega)|^2 = (\sqrt{2\pi\sigma_t}e^{-\frac{\sigma_t}{2}(\delta\omega)^2})^2(2\pi\sigma_s)^3, \tag{A.11}$$

$$|G_{\text{boundary}_{(t)}}(\delta\omega)|^2 = \left|\sqrt{\frac{2\sigma_t}{\pi}}\frac{1}{-i\sqrt{\sigma}_t\delta\omega + 1}\right|^2(2\pi\sigma_s)^3,$$

but the space boundary term,

$$e^{-\sigma_s(\delta\vec{p})^2}|G_{\text{boundary}_{(s)}}(\delta\omega)|^2 = \left(\sqrt{\frac{2\sigma_t}{\pi}}\frac{1}{|-i\sqrt{\sigma}_t\delta\omega+1|}\sqrt{\frac{2\sigma_s}{\pi}}(2\pi\sigma_s)\right)^2 \times\left[\left|\frac{1}{-i\sqrt{\sigma}_s\delta p_z+1}\right|^2 e^{-\sigma_s((\delta\vec{p}_x)^2+(\delta\vec{p}_y)^2)}+|(x,y,z)|^2+|(y,z,x)|^2\right], \quad \text{(A.12)}$$

is different. The momentum dependence of the bulk term and that of the time boundary are spherically symmetric as before, but that of the space boundary is asymmetric.

A.3. Normalization of probability: summation over the positions

The integrations over the positions $\vec{X}_{\gamma l}$, over the position $\vec{X}_{e^+}$ in the region of L^3 and the time interval T, and for the boundary of the width $\sqrt{2\sigma_t}$ and $\sqrt{2\sigma_s}$ are:

$$\int d\vec{X}_{e^+}\int\frac{d\vec{X}_{\gamma_1}d\vec{X}_{\gamma_2}}{(2\pi)^6}e^{-2R(\vec{X}_{\gamma_i})}\theta(\vec{X}_\gamma,\text{volume}) = TL^3, \quad \text{(A.13)}$$

$$\int d\vec{X}_{e^+}\int\frac{d\vec{X}_{\gamma_1}d\vec{X}_{\gamma_2}}{(2\pi)^6}e^{-2R(\vec{X}_{\gamma_i})}\theta(\vec{X}_\gamma,\text{b}_t) = \frac{\sqrt{2\sigma_t}}{T}(TL^3), \quad \text{(A.14)}$$

$$\int d\vec{X}_{e^+}\int\frac{\int d\vec{X}_{\gamma_1}d\vec{X}_{\gamma_2}}{(2\pi)^6}e^{-2R(\vec{X}_{\gamma_i})}\theta(\vec{X}_\gamma,b_{s,t}) = \frac{\sqrt{2\sigma_t 2\sigma_s}}{TL}(TL^3). \quad \text{(A.15)}$$

Substituting these, we have the momentum distribution

$$\frac{1}{TL^3}\frac{dP}{d^3k_1d^3k_2} = \frac{2}{m^2}\left(1+\frac{1}{4}(1-\cos\theta)+\frac{1}{2}(\frac{m}{E_{\gamma_1}}+\frac{m}{E_{\gamma_2}})\right) \left[e^{-\sigma_s(\delta P)^2}\left(P_0^{\text{bulk}}|G_{\text{bulk}}(\delta\omega)|^2+P_0^{\text{b}_t}\left|G_{\text{boundary}_{(t)}}(\delta\omega)\right|^2\right) + P_0^{\text{b}_s}e^{-\sigma_s(\delta P)^2}\left|G_{\text{boundary}_{(s)}}(\delta\omega)\right|^2\right], \quad \text{(A.16)}$$

where Eqs. (A.22) and (A.12) are substituted, and

$$P_0^{\text{bulk}} = (E_{e^+}E_{\gamma_1}E_{\gamma_2})^{-1}C \qquad \text{bulk}, \quad \text{(A.17)}$$

$$P_0^{\text{b}_{(t)}} = (E_{e^+}E_{\gamma_1}E_{\gamma_2})^{-1}C\frac{\sqrt{2\sigma_t}}{T} \qquad \text{boundary in time}, \quad \text{(A.18)}$$

$$P_0^{\text{b}_{(s)}} = (E_{e^+}E_{\gamma_1}E_{\gamma_2})^{-1}C\frac{\sqrt{2\sigma_t 2\sigma_s}}{TL} \qquad \text{boundary in space}, \quad \text{(A.19)}$$

where C is a constant. In the present situation, the target is composed of silica particles of $L = 7$ nm, and it is reasonable to assume that $E_{e^+} = m_e(1\pm\frac{1}{10})$, $\frac{\sqrt{2\sigma_s}}{L}$, $\frac{\sqrt{2\sigma_t}}{T}\approx\frac{1}{10}-\frac{1}{100}$. The spectrum of the boundary term is of the universal form, but its magnitude has uncertainties due to the uncertainties on the wave packets. This ambiguity could be studied by a light scattering of the silica powder.

A.4. Non-Gaussian wave packet

The function $e^{-\mu r}$, where $r = |\vec{x}|$ and μ is a constant, decreases rapidly at large distance r but has a singularity at $r = 0$. Its Fourier transform is $\frac{1}{(p^2+\mu^2)^2}$, and decreases slowly in the momentum.

Accordingly, a wave packet of this form leads to a probability different from the Gaussian one. This is studied hereafter.

A.4.1. Amplitude

For non-Gaussian wave packets, the momentum-dependent amplitudes in the bulk and boundary terms are

$$M_{\text{bulk}} = f_0 \frac{\frac{2}{t_0}}{\omega^2 + (\frac{1}{t_0})^2} \times f_0 8\pi \frac{1}{r_0} \frac{1}{((\frac{1}{r_0})^2 + (\delta\vec{p})^2)^2} \theta(\vec{X}_\gamma, \text{volume}), \tag{A.20}$$

$$M_{\text{boundary}_{(t)}} = f_0 \frac{1}{i\omega + \frac{1}{t_0}} \times f_0 8\pi \frac{1}{r_0} \frac{1}{((\frac{1}{r_0})^2 + (\delta\vec{p})^2)^2} \theta(\vec{X}_\gamma, \text{b}_t), \tag{A.21}$$

where $f_0 = \frac{1}{\sqrt{\pi r_0^3}}$, and t_0 and r_0 are determined from the size of the Coulomb wave function; they are given for NaI at the end of this appendix. These lead to a probability of the same form as before:

$$|G_{\text{bulk}}(\delta\omega, \delta\vec{p})|^2 = \left[f_0 \frac{\frac{2}{t_0}}{\omega^2 + (\frac{1}{t_0})^2} \times f_0 8\pi \frac{1}{r_0} \frac{1}{((\frac{1}{r_0})^2 + (\delta\vec{p})^2)^2} \right]^2, \tag{A.22}$$

$$|G_{\text{boundary}_{(t)}}(\delta\omega, \delta\vec{p})|^2 = \left[f_0 \frac{1}{i\omega + \frac{1}{t_0}} \times f_0 8\pi \frac{1}{r_0} \frac{1}{((\frac{1}{r_0})^2 + (\delta\vec{p})^2)^2} \right]^2.$$

The integration over the positions $\vec{X}_{\gamma_l}$ and over the position $\vec{X}_{e^+}$ are also the same as before. We have the momentum distribution

$$\frac{1}{TL^3} \frac{dP}{d^3k_1 d^3k_2} = \frac{2}{m^2} \left(1 + \frac{1}{4}(1 - \cos\theta) + \frac{1}{2} \left(\frac{m}{E_{\gamma_1}} + \frac{m}{E_{\gamma_2}} \right) \right) \times \left[\left(P_0^{\text{bulk}} |G_{\text{bulk}}(\delta\omega, \delta\vec{p})|^2 + P_0^{\text{b}_t} \left| G_{\text{boundary}_{(t)}}(\delta\omega, \delta\vec{p}) \right|^2 \right) \right], \tag{A.23}$$

where Eqs. (A.22) and (A.12) are substituted, and

$$P_0^{\text{bulk}} = (E_{e^+} E_{\gamma_1} E_{\gamma_2})^{-1} C_{\text{Coul}} \qquad \text{bulk}, \tag{A.24}$$

$$P_0^{\text{b}_{(t)}} = (E_{e^+} E_{\gamma_1} E_{\gamma_2})^{-1} C_{\text{Coul}} \frac{\sqrt{2\sigma_t}}{T} \qquad \text{boundary},$$

where C_{Coul} is a constant which is related to C, $r_0 = \frac{\sqrt{\sigma_s}}{50}$, and $t_0 = \frac{\sqrt{\sigma_t}}{50}$. We leave C_{Coul} as a parameter for a while.

B. Duplicate (accidentally coincident and pile-up) events

Suppose the probability is a sum of duplicate (accidental coincident and pile-up) events and $P^{(d)}$ events:

$$f(p_1, p_2) = c_0 g(p_1) g(p_2) + g(p_1, p_2), \tag{B.1}$$

where $g(p_1)$ and $g(p_1,p_2)$ are known theoretically, but c_0 in experiments is unknown. Define an error function

$$\begin{aligned} I_{\rm error}(c) &= \int dp_1 dp_2 (f_{\rm exp}(p_1,p_2) - cg(p_1)g(p_2))^2 \\ &= \int dp_1 dp_2 [(c-c_0)^2 (g(p_1)g(p_2))^2 + (g(p_1,p_2))^2 - 2(c-c_0)g(p_1)g(p_1,p_2)g(p_2)] \\ &= (c-c_0)^2 A_2 - 2(c-c_0)A_1 + A_0 = A_2(c-\tilde{c}_0)^2 + A_0 - A_1^2/A_2, \end{aligned} \tag{B.2}$$

where

$$\begin{aligned} A_2 &= \int dp_1 dp_2 (g(p_1)g(p_2))^2, \\ A_1 &= \int dp_1 dp_2 g(p_1)g(p_1,p_2)g(p_2), \\ A_0 &= \int dp_1 dp_2 (g(p_1,p_2))^2. \end{aligned} \tag{B.3}$$

Plot $I_{\rm error}(c)$ as a function of c and obtain the minimum value $D = A_0 - A_1^2/A_2$,

$$D = -\left[\int dp_1 dp_2 g(p_1)g(p_1,p_2)g(p_2)\right]^2 / \int dp_1 dp_2 (g(p_1)g(p_2))^2 + \int dp_1 dp_2 g(p_1,p_2)^2. \tag{B.4}$$

For $P^{(d)} = 0$, $g(p_1,p_2) = 0$ and $D = 0$; for $P^{(d)} \neq 0$, $g(p_1,p_2) > 0$ and $D > 0$. Experimental determination of $D > 0$ may be feasible.

References

[1] P. A. M. Dirac and N. H. D. Bohr, Pro. R. Soc. Lond. A **114**, 243 (1927).
[2] L. I. Schiff, *Quantum Mechanics* (McGraw-Hill, New York, 1955).
[3] K. Ishikawa and K. Oda, Prog. Theor. Exp. Phys. **2018**, 123B01 (2018) [arXiv:1809.04285 [hep-ph]] [Search INSPIRE].
[4] C. Patrignani, K. Agashe, G. Aielli, C. Amsler, M. Antonelli, D. M. Asner, H. Baer, Sw. Banerjee, and R. M. Barnett et al., [Particle Data Group], Chi. Phys. C, **40**, 100001 (2016), and the 2017 update.
[5] H. Fukuda and Y. Miyamoto, Prog. Theor. Phys. **4**, 235 (1949).
[6] J. Steinberger, Phys. Rev. **76**, 1180 (1949).
[7] S. Adler, Phys. Rev. **177**, 2426 (1969).
[8] J. S. Bell and R. Jackiw, Nuovo Cim. A **60**, 47 (1969).
[9] A. M. Bernstein and B. R. Holstein, Rev. Mod. Phys. **85**, 49 (2013).
[10] E. C. G. Stueckelberg, Phys. Rev. **81**, 130 (1951).
[11] M. L. Goldberger and K. M. Watson, *Collision Theory* (John Wiley & Sons, Inc., New York, 1965).
[12] R. G. Newton, *Scattering Theory of Waves and Particles* (Springer-Verlag, New York, 1982).
[13] J. R. Taylor, *Scattering Theory: The Quantum Theory of Non-relativistic Collisions* (Dover Publications, New York, 2006).
[14] K. Ishikawa and T. Shimomura, Prog. Theor. Phys. **114**, 1201 (2005) [arXiv:hep-ph/0508303] [Search INSPIRE].
[15] K. Ishikawa and Y. Tobita, Prog. Theor. Exp. Phys. **2013**, 073B02 (2013).
[16] K. Ishikawa and Y. Tobita, Ann. Phys. **344**, 118 (2014).
[17] K. Ishikawa, T. Tajima, and Y. Tobita, Prog. Theor. Exp. Phys. **2015**, 013B02 (2015).
[18] R. Peierls, *Surprises in Theoretical Physics* (Princeton University Press, Princeton, NJ, 1979), p. 121.
[19] H. Lehman, K. Symanzik, and W. Zimmermann, Nuovo Cim. **1**, 205 (1955).
[20] F. E. Low, Phys. Rev. **97**, 1392 (1955).
[21] V. Weisskopf and E. P. Wigner, Z. Phys. **63**, 54 (1930).

[22] V. Weisskopf and E. Wigner, Z. Phys. **65**, 18 (1930).
[23] J. Liu, Phys. Rev. D **44**, 2879 (1991).
[24] L. Stodolsky, Phys. Rev. D **58**, 036006 (1998) [arXiv:hep-ph/9802387] [Search INSPIRE].
[25] H. J. Lipkin, Phys. Lett. B **642**, 366 (2006) [arXiv:hep-ph/0505141] [Search INSPIRE].
[26] E. K. Akhmedov, J. High Energy Phys. **0709**, 116 (2007) [arXiv:0706.1216 [hep-ph]] [Search INSPIRE].
[27] K. Ishikawa and Y. Tobita, Prog. Theor. Phys. **122**, 1111 (2009) [arXiv:0906.3938 [quant-ph]] [Search INSPIRE].
[28] N. Maeda, T. Yabuki, Y. Tobita, and K. Ishikawa, Prog. Theor. Exp. Phys. **2017**, 053J01 (2017).
[29] F. Rohrich and B. C. Carson, Phys. Rev. **93**, 38 (1954).
[30] I. Hossain, N. Sharip, and K. K. Viswanathan, Sci. Res. Essays **7**, 86 (2012).
[31] M. Moszyski, J. Zalipska, M. Balcerzyk, M. Kapusta, W. Mengesha, and J. D. Valentine, Nucl. Instrum. Meth. Phys. Res. A **484**, 259 (2002).
[32] S. Agostinelli, J. Allison, K. Amako, J. Apostolakis, H. Araujo, P. Arce, M. Asai, D. Axen, S. Banerjee, and G. Barrand et al., Nucl. Instrum. Meth. A **506**, 250 (2003).
[33] S. Tanuma, C. J. Powell, and D. R. Penn, J. Appl. Phys. **103**, 063707 (2008).
[34] J. Cizek, M. Vlček, F. Lukáč, O. Melikhova, I. Procházka, W. Anwand, A. Wagner, M. Butterling, and R. Krause-Rehberg, J. Phys.: Conf. Ser. **505**, 012043 (2014).
[35] H. A. Bethe and R. H. Fowler, Proc. Roy. Soc. London, Ser. A: Math. Phys. Sci. **150**, 129 (1935).